Biomaterials 31 (2010) 1875–1884

Contents lists available at ScienceDirect

Biomaterials

journal homepage: www.elsevier.com/locate/biomaterials

Probing cellular mechanobiology in three-dimensional culture with collagen–agarose matrices

Theresa A. Ulrich [a,b], Amit Jain [a,1], Kandice Tanner [a], Joanna L. MacKay [a,c], Sanjay Kumar [a,b,*]

[a] Department of Bioengineering, University of California, Berkeley, CA 94720-1762, USA
[b] University of California, San Francisco/University of California, Berkeley Joint Graduate Group in Bioengineering, Berkeley, CA 94720, USA
[c] Department of Chemical Engineering, University of California, Berkeley, CA 94720, USA

ARTICLE INFO

Article history:
Received 28 September 2009
Accepted 20 October 2009
Available online 18 November 2009

Keywords:
Hydrogel
Collagen
ECM (extracellular matrix)
Mechanical properties
Elasticity
Brain

ABSTRACT

The study of how cell behavior is controlled by the biophysical properties of the extracellular matrix (ECM) is limited in part by the lack of three-dimensional (3D) scaffolds that combine the biofunctionality of native ECM proteins with the tunability of synthetic materials. Here, we introduce a biomaterial platform in which the biophysical properties of collagen I are progressively altered by adding agarose. We find that agarose increases the elasticity of 3D collagen ECMs over two orders of magnitude with modest effect on collagen fiber organization. Surprisingly, increasing the agarose content slows and eventually stops invasion of glioma cells in a 3D spheroid model. Electron microscopy reveals that agarose forms a dense meshwork between the collagen fibers, which we postulate slows invasion by structurally coupling and reinforcing the collagen fibers and introducing steric barriers to motility. This is supported by time lapse imaging of individual glioma cells and multicellular spheroids, which shows that addition of agarose promotes amoeboid motility and restricts cell-mediated remodeling of individual collagen fibers. Our results are consistent with a model in which agarose shifts ECM dissipation of cell-induced stresses from non-affine deformation of individual collagen fibers to bulk-affine deformation of a continuum network.

1. Introduction

The behavior of many mammalian cell types is exquisitely sensitive to biophysical signals from the extracellular matrix (ECM), including those encoded within matrix mechanical properties [1]. The robust mechanosensitivity of mammalian cells has been extensively probed in vitro using two-dimensional (2D) biomaterial platforms that feature full-length ECM proteins covalently conjugated to polymeric hydrogels of defined stiffness [2], thus allowing independent modulation of ECM mechanical and biochemical properties. We and others have used these platforms to demonstrate that cellular structure, motility, and proliferation can be strongly regulated by the mechanical rigidity of the ECM [2,3]. However, many cells reside in a three-dimensional (3D) ECM in vivo, and it is now well-established that culture dimensionality strongly impacts gene expression, cell adhesion and migration, and assembly into multicellular structures [4,5].

Although there is increasing interest in investigating cellular mechanobiological properties in 3D culture systems, the development of matrices for this purpose has proven challenging. One common strategy is based on incorporation of cell adhesion peptides (e.g., RGD) into synthetic polymer networks [6–8]; while this frequently offers robust and independent control of ECM ligand density and mechanics, it necessarily sacrifices the rich biochemical and topological information encoded in networks of full-length matrix proteins. Conversely, strategies that control 3D matrix properties by varying the concentration of a native ECM formulation (e.g., collagen, Matrigel) access a fairly narrow stiffness range due to the intrinsically low elasticity of most of these materials and concurrently change ECM mechanics, ligand density, microstructure, and other potentially confounding biophysical parameters [9,10].

Collagen I is both the most abundant ECM protein in mammalian tissues and one of the most widely-used scaffolds for three-dimensional cell culture and tissue engineering applications, which is partly derived from the ability of purified collagen I monomers to self-assemble into stable, three-dimensional gels at physiological

* Corresponding author. Department of Bioengineering, University of California, Berkeley, CA 94720-1762, USA. Tel.: +1 510 643 0787; fax: +1 510 642 5835.
E-mail address: skumar@berkeley.edu (S. Kumar).
[1] Present address: Amit Jain's present address is Johns Hopkins University School of Medicine, Baltimore, Maryland 21205.

0142-9612/$ – see front matter © 2009 Elsevier Ltd. All rights reserved.
doi:10.1016/j.biomaterials.2009.10.047

temperature and pH [4]. Gelation begins with the entropy-driven nucleation of triple-helical collagen monomers into small aggregates, which subsequently self-assemble into thin filaments that laterally crosslink into collagen fibers. A three-dimensional matrix is then formed via non-covalent entanglement of the fibers [4]. As a consequence of this entanglement, reconstituted collagen networks typically exhibit non-affine mechanical properties; i.e., applied stresses are dissipated non-uniformly throughout the gel via the sliding, slipping, bending, and buckling of individual collagen fibers [11]. Indeed, this non-affine stress dissipation is a near-universal property of native ECM formulations and contributes to the strongly nonlinear elastic properties of these matrices in bulk, which may provide an important source of mechanical reinforcement when these matrices are loaded in vivo [12,13].

The fiber diameter, pore size, and bulk elasticity of reconstituted collagen gels can be tuned within modest ranges by changing collagen concentration, ionic strength, pH, and the temperature of gelation [4,14]. Although matrix stiffness is most commonly varied by changing collagen concentration, even modest changes in the concentration of collagen monomers can significantly influence gelation kinetics, fiber diameter, fiber number, and porosity, in addition to increasing the number of integrin-binding sites, as described earlier [14]. To circumvent these limitations, a variety of approaches have been developed to crosslink collagen ECMs, including UV or gamma irradiation [15,16], enzymatic or chemical crosslinking [17–20], and nonenzymatic glycation or nitration [21,22]. More recently, crosslinking mechanisms utilizing the plant extract genipin [23] or multifunctional dendrimers [24] have been used to stiffen collagen matrices. However, speed, cost, and cytotoxicity continue to pose significant experimental limitations; for example, irradiation and chemical crosslinking can be highly cytotoxic, glycation often requires weeks, and the use of enzymes such as lysyl oxidase or transglutaminase can be prohibitively expensive [23].

Agarose, a neutral, galactopyranose-based linear polysaccharide, is a biocompatible and readily-available material that potentially offers a much wider dynamic range of biophysical properties than collagen [25]. Gelation of a homogeneous agarose solution occurs according to a coil-helix transition that begins when the solution is cooled to the ordering temperature (typically ~35 °C) where random coils of agarose begin forming single or double helices in solution. These helices aggregate to form an ordered structure of bundled double helices connected by flexible chains [26]. The physical and mechanical properties of agarose gels have been studied in considerable detail over the past 30 years, showing that the final gel structure tends to be isotropic with an average porosity of approximately 100–300 nm [27,28]. Agarose also has a number of attractive properties for biomaterial applications, in that it is inexpensive, non-toxic, inert to mammalian cell adhesion and degradation, and stiffens over several orders of magnitude for only modest increases in concentration [25]. Indeed, 3D agarose hydrogels have proven valuable as a culture scaffold for a variety of tissue engineering applications that do not require provision of a bioactive ECM [29,30]. Moreover, recent studies have suggested that agarose can be incorporated into networks of collagen I, which has generated interest in the potential utility of these composites in tissue engineering and 3D cell culture applications [31–34].

Given these properties, and given the need for 3D matrix systems that combine the biofunctionality of native ECM formulations with the tunability and dynamic range of synthetic scaffolds, we asked whether we might be able to vary the biophysical properties of collagen I matrices in a graded fashion by adding defined concentrations of agarose. In this study, we systematically vary the agarose content of collagen–agarose scaffolds in order to create a simple, inexpensive material platform in which ECM biophysical properties can be tuned independently of collagen content in 3D. We measure gel elasticity using parallel plate rheometry and characterize matrix structure using a combination of light and electron microscopy. We then use a series of collagen–agarose gels with increasing stiffness to study the mechanosensitivity of glioblastoma multiforme (GBM) cells, a system we have previously shown to be highly sensitive to ECM-based biophysical cues in 2D culture [3].

2. Materials and methods

2.1. Preparation of collagen–agarose gels

Stock 1.5 mg/ml collagen solutions were prepared on ice immediately prior to use by diluting PureCol (3 mg/ml sterile pepsin-solubilized bovine collagen in solution, ~97% collagen I, 3% collagen III; Advanced Biomatrix, San Diego, CA) in Dulbecco's Modified Eagle Medium (DMEM, Life Technologies, Grand Island, NY); 1 M NaOH was added to bring the pH to 7.4. Stock agarose solutions were prepared by dissolving 2% w/v low melting temperature agarose (A9414 supplied with sulfate content <0.1%; Sigma–Aldrich, St. Louis, MO) in DMEM and adjusting the pH to 7.4; the solution was then brought to 95 °C in a water bath prior to use. Collagen–agarose gels were prepared by combining collagen and agarose stock solutions with additional DMEM in appropriate volumes to create 0.5 mg/ml collagen gels with agarose concentrations ranging from 0–1% w/v. Solutions were mixed thoroughly prior to dispensing into cell culture or rheology dishes. Substrates were incubated at 37 °C for 1 h prior to addition of a superlayer of cell culture medium.

2.2. Characterization of mechanical properties

All rheology measurements were taken with an Anton Paar Physica MCR-300 or 301 rheometer (Anton Paar USA, Temecula, CA) at 37 °C and high humidity using a 25 mm parallel plate geometry and Rheoplus software. Preliminary amplitude sweeps over the range $\gamma = 0.1$–10% were used to identify the linear regime; frequency sweeps at 5% strain over the range 0.1–10 Hz were then used to extract the storage modulus, loss modulus, and complex modulus of each sample. At least five independent samples were measured for each gel formulation; reported storage moduli represent mean ± SEM at 0.4 Hz. Representative amplitude and frequency sweeps for different gel formulations are provided in Supplementary Fig. 1.

2.3. Cell culture and preparation of glioma spheroids

U373-MG human glioma cells were obtained from the Tissue Culture Facility at the University of California, Berkeley and cultured in DMEM supplemented with 10% Calf Serum Advantage (J.R. Scientific, Woodland, CA) and 1% penicillin/streptomycin, MEM nonessential amino acids, and sodium pyruvate (Life Technologies). Multicellular tumor spheroids were created using the hanging drop method [35,36]. Briefly, droplets of cell suspension containing ~500 cells were plated on the lid of a petri dish, inverted, and cultured over a dish of cell culture medium for 3 days. Spheroids of ~150 μm in diameter were manually collected using a micropipette and implanted in collagen–agarose substrates prior to gelation.

2.4. Microscopy and measurement of spheroid invasion

Simultaneous confocal reflectance and second harmonic generation (SHG) images were obtained using a Zeiss LSM 510/NLO META by exciting the sample with 800 nm from a Spectra-Physics MaiTai HP laser at a power of <25% of the maximum power as well as 488 nm from an argon ion laser at a power of <1% of total power (~0.3 mW). The META detector of the instrument was used in the emission pathway, where the detector range was set to 390–410 nm to obtain the SHG signal while the Zeiss was operated with no band pass filter so that all the light reflected was detected by the photomultiplier tube. We employed a 63× oil objective with NA 1.3 to obtain images of 512 × 512 pixels (133.6 μm × 133.6 μm) at a scan speed of ~1 sec/frame. DIC and phase contrast microscopy were performed using an inverted Nikon TE2000-E2 microscope equipped with a motorized, programmable stage (Prior Scientific, Inc, Rockland, MA), an incubator chamber to maintain constant temperature, humidity, and CO_2 levels (In Vivo Scientific, St. Louis, MO), a digital camera (Photometrics CoolSNAP HQ II, Roper Scientific, Tucson, AZ), and SimplePCI software (Hamamatsu Corporation, Sewickley, PA). Quantification of spheroid invasion was performed in SimplePCI by quantifying the total area occupied by cells in time lapse 10× phase contrast images captured through the mid-plane of each spheroid. Values were normalized to the initial area, such that the area is 100% for $t = 0$.

2.5. Electron microscopy

Collagen–agarose solutions were incubated at 37 °C at high humidity for 1 h on silicon wafers. Gels were fixed in 2% glutaraldehyde overnight at 4 °C and 1% osmium tetroxide for 1 h at room temperature (both in 0.1 M sodium cacodylate buffer, pH 7.2) prior to dehydration in an ethanol series, critical-point drying (AutoSamdri 815, Tousimis, Rockville, MD), sputter coating with 1–2 nm of gold and palladium (Tousimis), and examination with a Hitachi S-5000 scanning electron microscope at 3000×, 10,000× and 30,000× magnification.

3. Results

3.1. Gel elasticity and structure

We began by synthesizing a series of collagen–agarose hydrogels in which we fixed the collagen concentration at 0.5 mg/ml and varied the agarose concentration from 0 to 1% w/v, and we asked whether addition of agarose could progressively alter gel elastic properties while preserving collagen fiber architecture. Parallel plate rheometry revealed that the macroscopic storage modulus of collagen increased by over two orders of magnitude as the agarose concentration was increased from 0–1% w/v (Fig. 1), with the highest agarose concentrations yielding storage moduli approaching 1 kPa. This value is more than an order of magnitude greater than we could achieve with pure collagen gels, even by tripling the collagen concentration to 1.5 mg/ml (Supplementary Fig. 2A). Visualization of these collagen–agarose gels using Nomarski DIC imaging, confocal reflectance microscopy, and SHG imaging all failed to reveal gross alterations in apparent collagen fiber diameter or architecture up to 0.25% w/v agarose, with moderate differences becoming clear only for gels with agarose content of 0.5% w/v or higher (Fig. 2). This is in stark contrast to pure collagen gels stiffened by increasing collagen concentration from 0.5 mg/ml to 1.5 mg/ml (Supplementary Fig. 2B; [14,37–39]).

3.2. Glioma cell invasion

Previously, we have shown that increasing ECM elasticity in 2D could speed the random motility of a panel of glioma cell lines, including U373-MG cells. Therefore, we next used our collagen–agarose gel platform to ask how variation in the agarose content of 0.5 mg/ml collagen gels might influence glioma cell invasion in the context of 3D ECMs. For these studies, we used a spheroid invasion model in which cells are grown as multicellular spheroids in hanging-drop culture and implanted into the gel during the gelation process, such that the gel forms around the spheroid [36]. Over time, cells migrate away from the spheroid into the surrounding matrix, and invasion may be tracked by measuring the total projected area occupied by cells throughout the matrix. Time lapse phase contrast microscopy revealed a dramatic inhibition of spheroid invasion as the concentration of agarose was increased, including complete abolition of invasion in gels containing 1% w/v agarose (Fig. 3, Supplementary Movies 1–3). This is in stark contrast to pure collagen gels stiffened by increasing collagen concentration, where gel stiffness did not directly correlate with invasiveness (Supplementary Fig. 2C and D), as has been reported by others [36]. Importantly, pure agarose gels did not support cellular invasion at any concentration in the absence of collagen, demonstrating that adhesive cues from the collagen are both necessary and sufficient for motility (Supplementary Fig. 3). Based on these results, we surmised that increasing ECM rigidity apparently exerted the opposite effect in 2D and 3D, enhancing motility in the former case and inhibiting it in the latter.

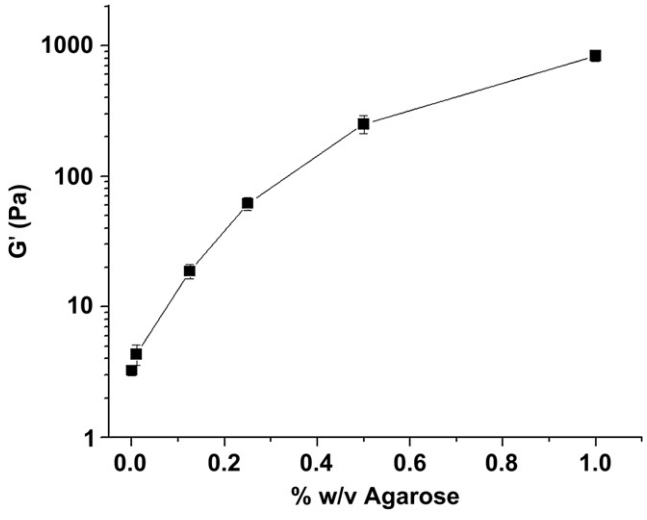

Fig. 1. Effect of agarose on storage modulus of collagen gels. Parallel-plate rheometric measurements of the bulk storage (elastic) modulus (G′) of 0.5 mg/ml collagen gels in the presence of 0–1% w/v agarose. Each data point represents mean ± SEM for n ≥ 5 samples.

3.3. Gel porosity

The above results imply that addition of agarose to collagen I matrices increases stiffness and reduces cell motility in 3D, but does so through a mechanism that does not primarily involve substantial changes in collagen ligand density or fiber architecture. Given that agarose had only a modest influence on collagen fiber organization, we hypothesized that the dramatic inhibition of glioma invasion might result from steric hindrance, where the increasing agarose content reduced the mesh size of the ECM, which would in turn progressively restrict the movement of both individual collagen fibers and glioma cells. This would also help reconcile the disparity between rigidity effects in 2D and 3D, as cells migrating in 2D culture need not overcome steric barriers in order to migrate. To test this hypothesis and gain additional insight into potential microstructural effects, we used SEM imaging to directly visualize the collagen and agarose. These studies revealed that agarose forms an intercalating matrix between the collagen fibers with a fine web-like architecture (Fig. 4) similar to the agarose structure reported by others [40] and consistent with the notion that agarose creates steric barriers to motility. Moreover, collagen fiber diameters observed by SEM were in good agreement with those observed by DIC, reflectance, and SHG imaging (Fig. 1; [37–39]) and provided further confirmation that fiber diameter is largely independent of agarose concentration.

3.4. Mesenchymal-amoeboid transition

Such dramatic changes in gel porosity would be expected to trigger a mesenchymal-amoeboid transition (MAT), in which cell migration transforms from a "mesenchymal" mode of motility characterized by an elongated morphology with established cell polarity and proteolytic degradation of the surrounding matrix to an "amoeboid" mode of motility characterized by a rounded morphology and propulsive, contractility-dependent squeezing through pre-existing pores in the matrix [41–43]. Indeed, high-resolution time lapse imaging of single glioma cells migrating through 3D collagen–agarose matrices showed strong evidence for a progressive MAT as the agarose content was increased (Fig. 5, Supplementary Movies 4–6). Cells in agarose-poor gels were often elongated and moved in a directionally-persistent fashion, whereas cells in agarose-rich gels extended thin projections in many directions at the leading edge and exhibited multiple constriction

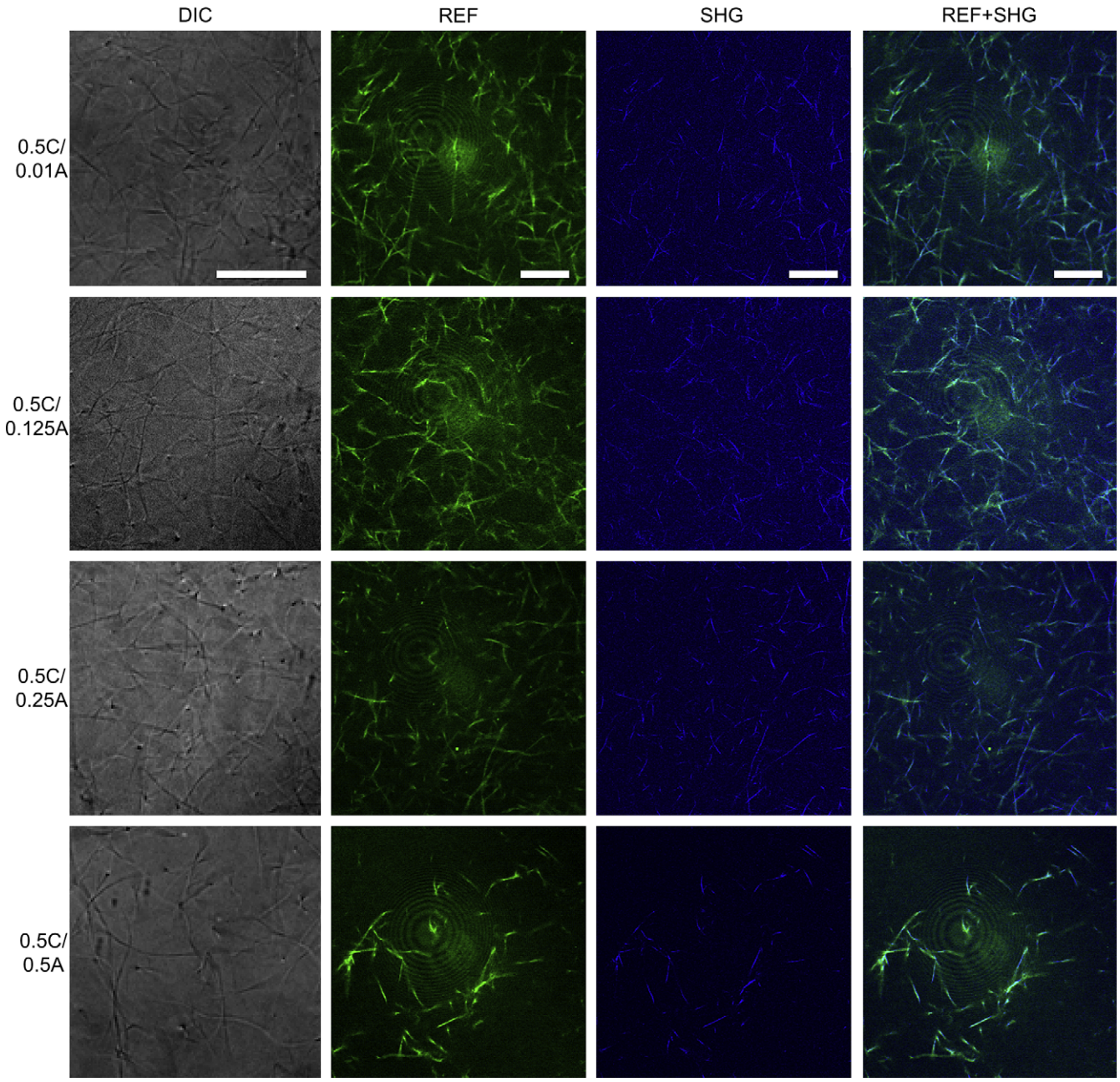

Fig. 2. Effect of agarose on collagen fibril architecture. High-magnification differential interference contrast (DIC), confocal reflectance (REF) and second harmonic generation (SHG) imaging of collagen fiber microarchitecture within collagen–agarose composite gels containing 0.5 mg/ml collagen (0.5 C) and 0.01–0.5% w/v agarose (0.01A – 0.5A). DIC and REF images are representative of $n \geq 3$ samples per condition; REF + SHG images were captured simultaneously and are representative of multiple images acquired from within a single gel sample. Bar = 25 μm.

rings along the cell body as the cells squeezed through pores in the matrix.

3.5. Collagen fiber deformability

Mesenchymal motility in collagen matrices is associated with successive deformation and relaxation of individual collagen fibers [41]. Thus, we reasoned that an additional mechanistic origin of the observed MAT might be that addition of agarose restricts the deformability of individual collagen fibers. To visualize these potential differences directly and in the complete absence of 3D steric barriers, we next cultured glioma cells on the surface of collagen–agarose gels and obtained phase contrast and DIC time lapse images of cell motility. After 24 h, cells plated on the surface of relatively thick gels (>1 mm) showed dramatic differences in cell morphology and organization (Fig. 6A). Specifically, cells plated on agarose-poor gels were elongated and visibly aligned with collagen fiber bundles, whereas cells plated on agarose-rich gels were rounded and tended to form spherical aggregates, consistent with a restricted ability to access and remodel the collagen fibers into larger bundles.

Additional insight into this phenomenon came from high-magnification time lapse DIC imaging of cells plated on the surface of thin gels (50–100 μm), which allowed visualization of the dramatic differences in collagen fiber bundling (Fig. 6B) and revealed intriguing differences in the mechanisms through which cells interact with collagen fibers as the agarose content of the gels is increased (Fig. 6C,D, Supplementary Movies 7 and 8). In pure

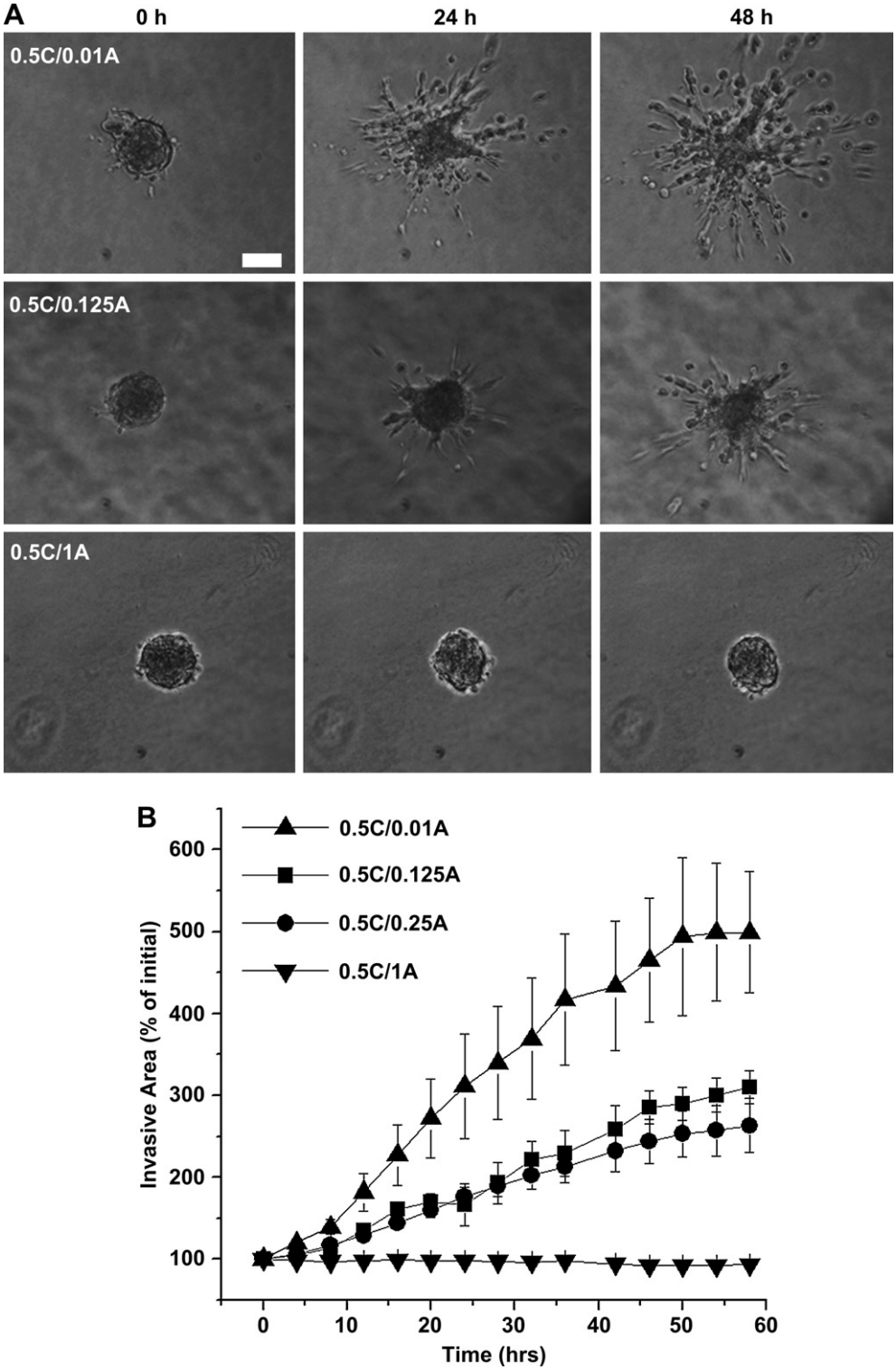

Fig. 3. Control of 3D cell motility by agarose content. Glioma cell invasion from spheroids into collagen–agarose gels is progressively restricted by the presence of agarose. A. Time lapse images of spheroid invasion in gels composed of 0.5 mg/ml collagen (0.5 C) and 0.01–1% w/v agarose (0.01A–1A). Images depict the gel/spheroid sample with the median final invasive area for a given gel formulation. Bar = 100 μm. B. Quantification of the total spheroid cross-sectional area as a function of time. Data represent mean ± SEM for $n \geq 3$ spheroids per condition.

collagen or agarose-poor matrices, we primarily observed non-affine bending and slipping of individual collagen fibers in response to cell-induced stresses. In contrast, cells on agarose-rich gels appeared to deform the matrix as a continuum structure, with deformations of individual collagen fibers very strongly coupled to the deformations of surrounding fibers.

Revisiting the effects of agarose on microscale matrix remodeling in 3D spheroidal culture, we found that we could observe these differences particularly clearly by obtaining time lapse imaging of spheroid pairs that were fortuitously implanted in close proximity to one another (Fig. 6E, Supplementary Fig. 4). In pure collagen gels, spheroids initially located over a millimeter apart

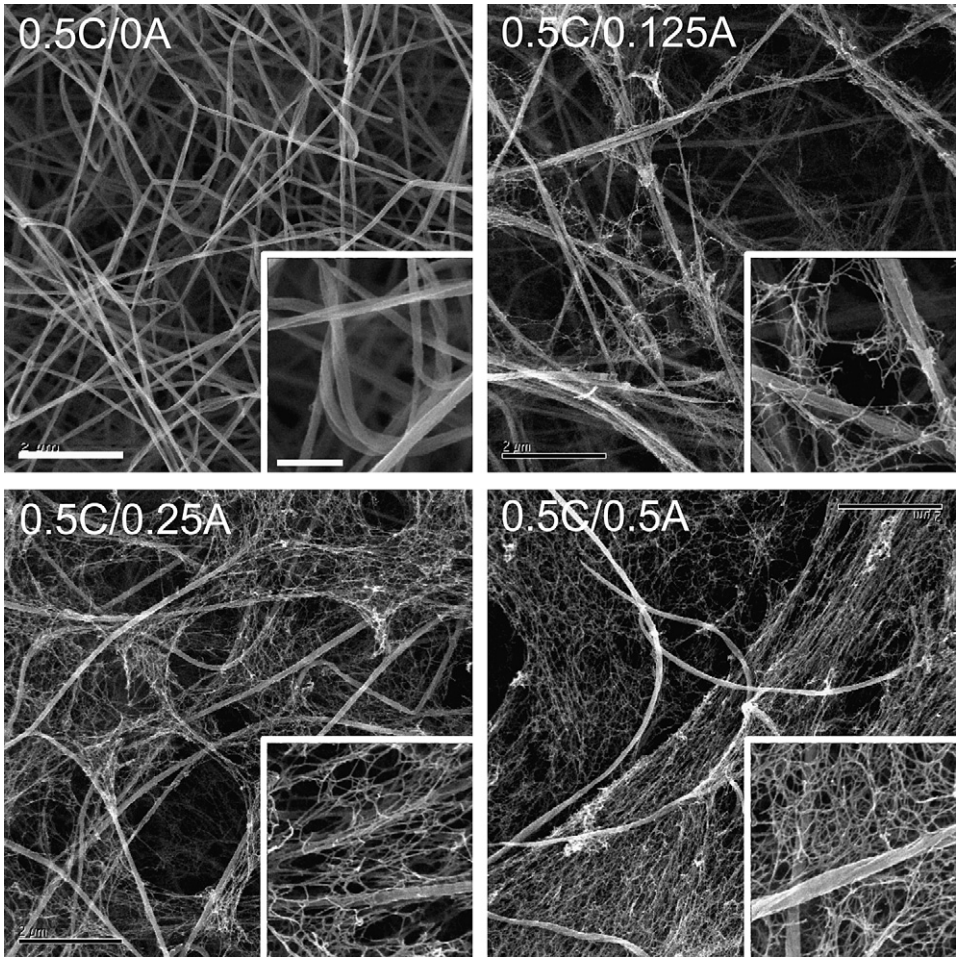

Fig. 4. Scanning electron microscopy imaging of collagen–agarose gels. SEM reveals that agarose forms an intercalating web-like network between the entangled collagen fibers that becomes progressively denser as the concentration of agarose is increased from 0 to 0.5% w/v agarose (0A–0.5A) in a 0.5 mg/ml collagen gel (0.5 C). Note that dehydration during SEM sample processing can give rise to an artifactual variation in the apparent density of collagen fibers at the surface of each gel sample. Bar = 2 μm (main panels) and 500 nm (insets).

were capable of mutually remodeling the ECM between them, ultimately creating bundles of fibers that served as contact guidance cues for trans-spheroid motility. Both the ECM remodeling and directional motility were significantly reduced in collagen/agarose matrices and completely absent in pure agarose matrices, even for spheroids initially located $<$300 μm (in this case, less than one spheroid diameter) from one another. In other words, addition of agarose inhibits the ability of cells to communicate mechanical signals to one another through the gel via remodeling of intervening matrix fibers.

4. Discussion

We have developed a strategy for modulating the biophysical properties of collagen gels in a graded fashion based on the incorporation of agarose, and we have shown that this approach is capable of fortifying the elasticity of weak collagen gels over two orders of magnitude without grossly disrupting fiber architecture. The addition of agarose also substantially inhibits cell invasion into the matrix and induces a transition from mesenchymal to amoeboid motility. This is consistent with a model in which agarose creates steric barriers to adhesion and motility and restricts cell-induced deformation and remodeling of the matrix, thus converting matrix rheology from a non-affine regime in which cell-induced loads are dissipated via the bending and slipping of individual collagen fibers to a bulk-affine regime in which the available degrees of freedom for individual fiber deformation is restricted and the movement of neighboring fibers appears coupled. One consequence of the cells' reduced ability to deform and remodel individual ECM fibrils is abrogation of topological communication between multicellular spheroids separated by only hundreds of micrometers.

Our findings bear at least two levels of significance. First, our material system combines the rich topological and biochemical information encoded in full-length, native ECM proteins with the wide biophysical dynamic range of agarose, which offers an alternative to the common practice of controlling the biophysical properties of native ECM formulations simply by varying ECM concentration. In doing so, our work adds to the small but growing repository of such hybrid materials [44–48] without requiring chemical conjugation of component precursors. Second, our results illustrate the inherent challenge–and instructiveness–of translating biophysical regulatory principles from 2D ECMs to 3D ECMs, in the sense that scaffold parameters not widely considered central to 2D motility, such as mesh size and fiber deformation, ultimately play critical roles in governing 3D motility. This lesson comes in the context of a recent surge of interest in dissecting the relative contributions of 3D ECM biophysical parameters to cell motility [30,33,49,50] and supports the notion that these parameters are sometimes intimately coupled; in this case, for example, a change

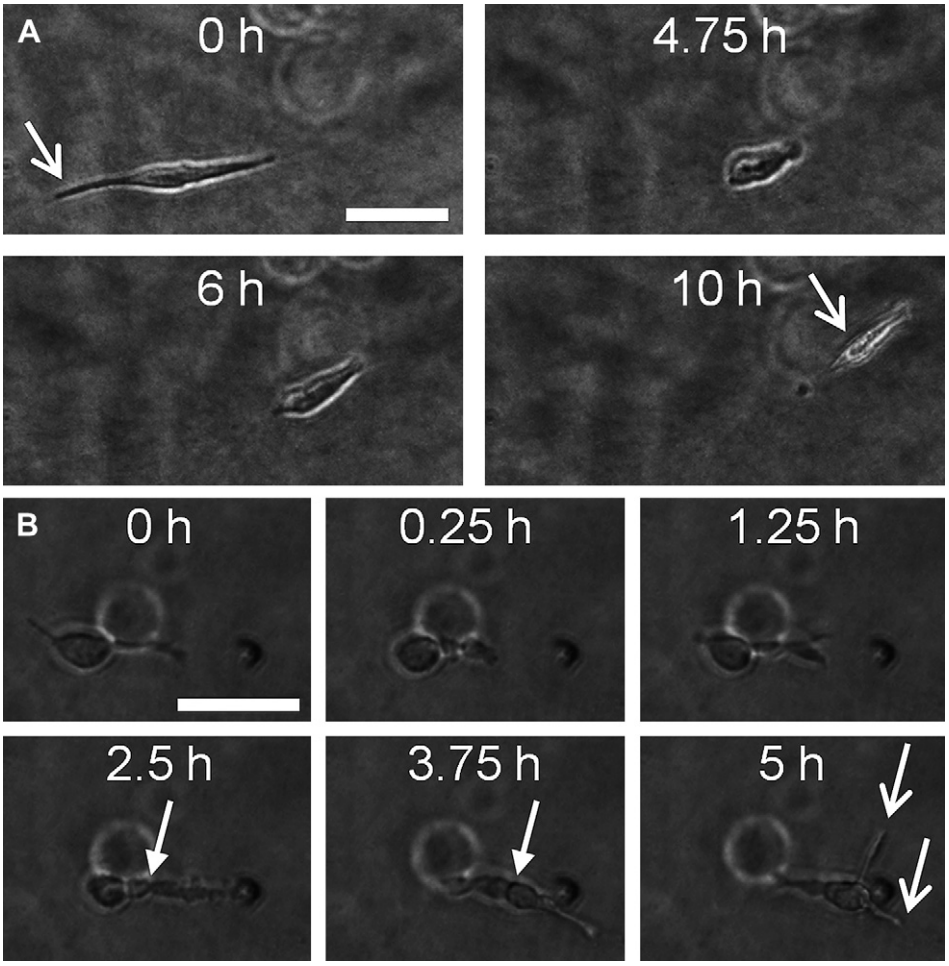

Fig. 5. Agarose-induced mesenchymal-to-amoeboid transition in cell motility. A. Motility in pure collagen gels. Cells in pure collagen gels are elongated (arrows) and migrate in a directionally-persistent, mesenchymal fashion. Similar motility was observed in agarose-poor gels (data not shown). B. Motility in agarose-rich gels. Cells embedded in 0.5 mg/ml collagen supplemented with 0.25% agarose exhibit a more rounded morphology and migrate in an amoeboid fashion, indicated by the presence of constriction rings (solid arrows) and active exploration of multiple migration paths at the leading edge (open arrows). Bar = 50 μm in both cases.

in elasticity is accompanied by a concurrent change in microstructure, and both appear to govern cell–matrix interactions during motility.

To expand on the latter point, the rigidity-dependence of cell spreading and motility in glioma cells on the surface of our collagen–agarose gels contrast with the rigidity-dependent behaviors we previously observed on polyacrylamide (pAA) gels [3]. Specifically, the high levels of glioma cell spreading and motility observed on the stiffest pAA gels ($G' \sim 40$ kPa) were severely restricted as matrix rigidity was decreased, where cells on the softest ($G' \sim 27$ Pa) pAA gels were uniformly rounded with limited motility. In contrast, glioma cell spreading and motility was restricted on the stiffest collagen–agarose gels ($G' \sim 835$ Pa) and progressively increased as matrix rigidity was decreased, where cells on the softest ($G' \sim 3$ Pa) gels were elongated and highly motile. This apparent contradiction is a consequence of the contrasting material properties of collagen and pAA. Collagen gels are comprised of entangled fibers that are known to impart non-affine mechanical properties [11,12]; as a result, we would expect cells in collagen matrices to generate long-range nonlinear matrix deformations and localized strain stiffening via non-uniform transmission of forces along individual collagen fibers or bundles. In contrast, pAA gels are linearly elastic; as a result, transmission of cell-generated forces should be homogeneous and therefore spatially limited. This phenomenology is in good agreement with recently-reported associations between the linear and nonlinear elastic properties of pAA and fibrin substrates, respectively, and differences in cell spreading, motility, and matrix deformability [13]. Finally, we would expect the presence of agarose in our collagen–agarose matrices to couple the collagen fibers together while restricting the available degrees of freedom for fiber bending, buckling and slipping. As a result, we expect that dissipation of cell-generated forces should transition from non-affine deformation of individual collagen fibers towards the bulk-affine deformation of a continuum network. This is consistent with the bulk-affine behavior that would be expected when the fibers in a non-affine matrix are made more resistant to bending [4].

We may also place our study in the context of earlier in vitro studies of glioma cell invasion and spheroid expansion [36,51,52]. In particular, Gordon et al. observed that expanding glioma spheroids exert both significant outward mechanical pressure and inward traction forces on the surrounding matrix [52]. In our system, we speculate that agarose may interfere with both of these processes; for example, the reduced mesh size of these gels prevents the intimate adhesion and spreading along collagen fibrils that would be needed to generate tractional forces, and the increased elastic modulus and conversion to bulk-affine mechanics may retard transmission of spheroid-generated compressive forces.

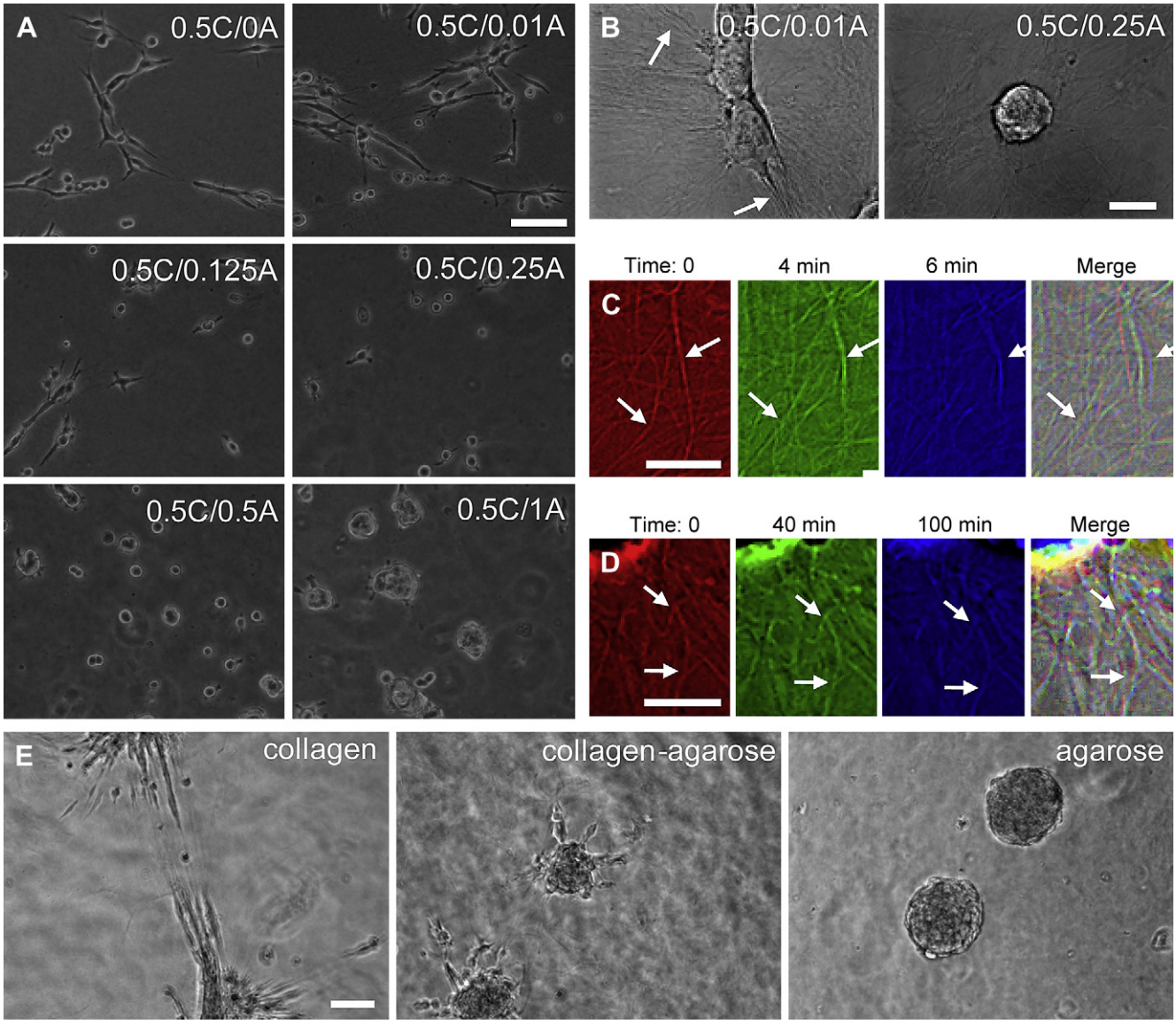

Fig. 6. Agarose-induced alterations in time scale and mechanism of stress dissipation. A. Phase contrast imaging of glioma cells on thick 2D collagen/agarose gels. Glioma cells cultured on the surface of 0.5 mg/ml collagen gels (0.5 C; gels are >1 mm in thickness) for 24 h are elongated and often organized into linear (end-to-end) patterns. As the concentration of agarose is increased from 0 to 1% w/v agarose (0A – 1A), cells become more rounded and form aggregates more readily. Bar = 100 μm. B. DIC imaging of cells on thin collagen/agarose gels. Glioma cells cultured on the surface of thin collagen–agarose gels (50–100 μm in thickness) are able to remodel the surrounding matrix to create bundles of aligned collagen fibers (arrows) when the matrix is agarose-poor. In contrast, even after 48 h, the collagen fibers in agarose-rich matrices are randomly aligned and resemble unseeded substrates. Bar = 25 μm. C, D. Differential matrix deformation dynamics in agarose-poor and agarose-rich gels. The images on the right (merge) depict a color overlay of DIC images obtained at the three time points on the left (red, green, and blue images) during high-magnification DIC time lapse imaging of the collagen fiber deformation generated by glioma cells cultured on the surface of thin collagen–agarose matrices (50–100 μm in thickness). C. Non-affine deformation in agarose-poor matrices. Individual collagen fibers in a 0.5 mg/ml collagen gel bear cell-imposed contractile stresses by slipping and bending (arrows) in divergent directions over short time scales. D. Bulk-affine deformation in a 0.5 mg/ml collagen gel supplemented with 0.25% w/v agarose. Individual collagen fibers appear to be coupled and deform over long time scales as a continuum substrate rather than a network of discrete entangled fibers, consistent with the expected decrease in the organizational entropy of individual collagen fibers. Bar = 10 μm for C and D. E. Topological communication between adjacent spheroids. The images depict invasion of cells from spheroids in close proximity 48 h post-implantation in matrices composed of pure collagen (left, 1.5 mg/ml), collagen/agarose (middle, 0.5 mg/ml collagen + 0.5% w/v agarose), and pure agarose (right, 0.5% w/v). A time lapse series is given in Fig. S4 in the Supporting Material. Bar = 100 μm.

This is strongly supported by our observation that reduction of agarose concentration promotes both invasion and apparent transmission of mechanical information through the matrix.

Our findings also have interesting connections to the recent work of Rosenfeld, Canoll, and colleagues, who found that under some conditions, glioma cell migration is rate-limited by the size of 3D matrix pores, and that below a critical pore size, these cells recruit nonmuscle myosin II (NMMII) to deform the nucleus and allow pore traversal [53]. This notion is consistent with our observation of MAT with increasing agarose concentration, because amoeboid motility is also accompanied by recruitment of myosin motors [54]. Thus, we would predict that repetition of these studies in the setting of NMMII inhibition would abrogate amoeboid motility and impair cellular invasion into agarose-rich gels. Also, it is noteworthy that cellular invasion is abrogated in the absence of collagen at all agarose concentrations (Supplementary Fig. 3), suggesting that U373-MG cells cannot transition to a ligand-independent mode of motility as has been reported for other cell types [54]. Finally, the MAT we observe in agarose-rich gels is strikingly similar to a recent report of MAT in U87-MG glioma cells, in which

Yamazaki et al. examined the roles of RhoA and Rac1 signaling in cell migration through 3D collagen gels [42]. In this system, Rac1 signaling promoted mesenchymal motility via WAVE/Arp2/3-dependent formation of cellular protrusions and adhesions, whereas RhoA signaling promoted amoeboid motility via Rho/ROCK pathway-mediated actomyosin contractility. This is consistent with the classically-observed antagonistic relationship between Rho and Rac GTPases in 2D cell migration and begs the question of whether RhoA and Rac1 play similar regulatory roles in our system. Biochemical studies and live-cell cytoskeletal imaging should help to clarify this issue.

5. Conclusions

In summary, we have introduced a materials platform in which we can modulate the biophysical properties of collagen I matrices in a simple, straightforward, and cost-effective manner. By combining multiple ultrastructural characterization methods with high-resolution live-cell imaging, we have used this system to explore the interplay between mechanics, microstructure and motility in human glioma cells. We anticipate that the approaches described in this study may prove valuable for probing the invasive behavior of a wide variety of tumor cell systems and, more generally, for investigating the effect of biophysical signals encoded in 3D matrices on cellular mechanobiology.

Acknowledgements

We thank Dr. G. Min at the Electron Microscopy Laboratory at UC Berkeley for assistance with scanning electron microscopy, J. Pollock and Dr. K. Healy for technical assistance with rheology and assistance with equipment, and J. Dabritz (Anton Paar) and D. Leong (Technical Instruments) for assistance with equipment and software. TAU gratefully acknowledges the support of the UC Berkeley Graduate Division, National Science Foundation, and National Defense Science and Engineering Graduate Fellowships. S.K. gratefully acknowledges grant support from the University of California, Berkeley, the UC Cancer Research Coordinating Committee, the Arnold and Mabel Beckman Young Investigator Award, the NSF (CMMI 0727420), and the NIH Director's New Innovator Award (1DP2OD004213), a part of the NIH Roadmap for Medical Research.

Appendix. Supplementary data

Supplementary data associated with this article can be found in online version at, doi:10.1016/j.biomaterials.2009.10.047.

References

[1] Discher D, Dong C, Fredberg JJ, Guilak F, Ingber D, Janmey P, et al. Biomechanics: cell research and applications for the next decade. Ann Biomed Eng 2009;37(5):847–59.
[2] Discher DE, Janmey P, Wang YL. Tissue cells feel and respond to the stiffness of their substrate. Science 2005;310(5751):1139–43.
[3] Ulrich TA, Juan Pardo EM, Kumar S. The mechanical rigidity of the extracellular matrix regulates the structure, motility, and proliferation of glioma cells. Cancer Res 2009;69(10):4167–74.
[4] Pedersen JA, Swartz MA. Mechanobiology in the third dimension. Ann Biomed Eng 2005;33(11):1469–90.
[5] Pampaloni F, Reynaud EG, Stelzer EH. The third dimension bridges the gap between cell culture and live tissue. Nat Rev Mol Cell Biol 2007;8(10):839–45.
[6] Kim S, Healy KE. Synthesis and characterization of injectable poly(*N*-isopropylacrylamide-co-acrylic acid) hydrogels with proteolytically degradable cross-links. Biomacromolecules 2003;4(5):1214–23.
[7] Peyton SR, Raub CB, Keschrumrus VP, Putnam AJ. The use of poly(ethylene glycol) hydrogels to investigate the impact of ECM chemistry and mechanics on smooth muscle cells. Biomaterials 2006;27(28):4881–93.
[8] Seliktar D, Zisch AH, Lutolf MP, Wrana JL, Hubbell JA. MMP-2 sensitive, VEGF-bearing bioactive hydrogels for promotion of vascular healing. J Biomed Mater Res A 2004;68(4):704–16.
[9] Willits RK, Skornia SL. Effect of collagen gel stiffness on neurite extension. J Biomater Sci Polym Ed 2004;15(12):1521–31.
[10] Zaman MH, Trapani LM, Sieminski AL, Mackellar D, Gong H, Kamm RD, et al. Migration of tumor cells in 3D matrices is governed by matrix stiffness along with cell–matrix adhesion and proteolysis. Proc Natl Acad Sci U S A 2006;103(29):10889–94.
[11] Chandran PL, Barocas VH. Affine versus non-affine fibril kinematics in collagen networks: theoretical studies of network behavior. J Biomech Eng 2006;128(2):259–70.
[12] Storm C, Pastore JJ, MacKintosh FC, Lubensky TC, Janmey PA. Nonlinear elasticity in biological gels. Nature 2005;435(7039):191–4.
[13] Winer JP, Oake S, Janmey PA. Non-linear elasticity of extracellular matrices enables contractile cells to communicate local position and orientation. PLoS ONE 2009;4(7):e6382.
[14] Yang YL, Kaufman LJ. Rheology and confocal reflectance microscopy as probes of mechanical properties and structure during collagen and collagen/hyaluronan self-assembly. Biophys J 2009;96(4):1566–85.
[15] Hamed G, Rodriguez F. Gelation of dilute collagen solutions by ultraviolet light. J Appl Polym Sci 1975;19(12):3299–313.
[16] Inoue N, Bessho M, Furuta M, Kojima T, Okuda S, Hara M. A novel collagen hydrogel cross-linked by gamma-ray irradiation in acidic pH conditions. J Biomater Sci Polym Ed 2006;17(8):837–58.
[17] Orban JM, Wilson LB, Kofroth JA, El-Kurdi MS, Maul TM, Vorp DA. Crosslinking of collagen gels by transglutaminase. J Biomed Mater Res A 2004;68(4):756–62.
[18] Olde Damink LHH, Dijkstra PJ, Luyn MJA, Wachem PB, Nieuwenhuis P, Feijen J. Glutaraldehyde as a crosslinking agent for collagen-based biomaterials. J Mater Sci Mater Med 1995;6(8):460–72.
[19] Siegel RC. Collagen cross-linking. Synthesis of collagen cross-links in vitro with highly purified lysyl oxidase. J Biol Chem 1976;251(18):5786–92.
[20] Sheu MT, Huang JC, Yeh GC, Ho HO. Characterization of collagen gel solutions and collagen matrices for cell culture. Biomaterials 2001;22(13):1713–9.
[21] Girton TS, Oegema TR, Tranquillo RT. Exploiting glycation to stiffen and strengthen tissue equivalents for tissue engineering. J Biomed Mater Res 1999;46(1):87–92.
[22] Paik DC, Dillon J, Galicia E, Tilson MD. The nitrite/collagen reaction: non-enzymatic nitration as a model system for age-related damage. Connect Tissue Res 2001;42(2):111–22.
[23] Sundararaghavan HG, Monteiro GA, Lapin NA, Chabal YJ, Miksan JR, Shreiber DI. Genipin-induced changes in collagen gels: correlation of mechanical properties to fluorescence. J Biomed Mater Res A 2008;87(2):308–20.
[24] Duan X, Sheardown H. Crosslinking of collagen with dendrimers. J Biomed Mater Res A 2005;75(3):510–8.
[25] Normand V, Lootens DL, Amici E, Plucknett KP, Aymard P. New insight into agarose gel mechanical properties. Biomacromolecules 2000;1(4):730–8.
[26] Arnott S, Fulmer A, Scott WE, Dea IC, Moorhouse R, Rees DA. The agarose double helix and its function in agarose gel structure. J Mol Biol 1974;90(2):269–84.
[27] Barrangou LM, Daubert CR, Allen Foegeding E. Textural properties of agarose gels. I. Rheological and fracture properties. Food Hydrocolloids;20(2–3):184–195.
[28] Griess GA, Moreno ET, Easom RA, Serwer P. The sieving of spheres during agarose gel electrophoresis: quantitation and modeling. Biopolymers 1989;28(8):1475–84.
[29] Bellamkonda R, Ranieri JP, Aebischer P. Laminin oligopeptide derivatized agarose gels allow three-dimensional neurite extension in vitro. J Neurosci Res 1995;41(4):501–9.
[30] Balgude AP, Yu X, Szymanski A, Bellamkonda RV. Agarose gel stiffness determines rate of DRG neurite extension in 3D cultures. Biomaterials 2001;22(10):1077–84.
[31] Batorsky A, Liao J, Lund AW, Plopper GE, Stegemann JP. Encapsulation of adult human mesenchymal stem cells within collagen–agarose microenvironments. Biotechnol Bioeng 2005;92(4):492–500.
[32] Lin PW, Wu CC, Chen CH, Ho HO, Chen YC, Sheu MT. Characterization of cortical neuron outgrowth in two- and three-dimensional culture systems. J Biomed Mater Res B Appl Biomater 2005;75(1):146–57.
[33] Cullen DK, Lessing MC, LaPlaca MC. Collagen-dependent neurite outgrowth and response to dynamic deformation in three-dimensional neuronal cultures. Ann Biomed Eng 2007;35(5):835–46.
[34] Lund AW, Bush JA, Plopper GE, Stegemann JP. Osteogenic differentiation of mesenchymal stem cells in defined protein beads. J Biomed Mater Res B Appl Biomater 2008;87(1):213–21.
[35] Timmins NE, Nielsen LK. Generation of multicellular tumor spheroids by the hanging-drop method. Methods Mol Med 2007;140:141–51.
[36] Kaufman LJ, Brangwynne CP, Kasza KE, Filippidi E, Gordon VD, Deisboeck TS, et al. Glioma expansion in collagen I matrices: analyzing collagen concentration-dependent growth and motility patterns. Biophys J 2005;89(1):635–50.
[37] Raub CB, Suresh V, Krasieva T, Lyubovitsky J, Mih JD, Putnam AJ, et al. Noninvasive assessment of collagen gel microstructure and mechanics using multiphoton microscopy. Biophys J 2007;92(6):2212–22.
[38] Raub CB, Unruh J, Suresh V, Krasieva T, Lindmo T, Gratton E, et al. Image correlation spectroscopy of multiphoton images correlates with collagen mechanical properties. Biophys J 2008;94(6):2361–73.

[39] Mickel W, Munster S, Jawerth LM, Vader DA, Weitz DA, Sheppard AP, et al. Robust pore size analysis of filamentous networks from three-dimensional confocal microscopy. Biophys J 2008;95(12):6072–80.
[40] Dillon GP, Yu X, Sridharan A, Ranieri JP, Bellamkonda RV. The influence of physical structure and charge on neurite extension in a 3D hydrogel scaffold. J Biomater Sci Polym Ed 1998;9(10):1049–69.
[41] Wolf K, Mazo I, Leung H, Engelke K, von Andrian UH, Deryugina EI, et al. Compensation mechanism in tumor cell migration: mesenchymal-amoeboid transition after blocking of pericellular proteolysis. J Cell Biol 2003;160(2):267–77.
[42] Yamazaki D, Kurisu S, Takenawa T. Involvement of Rac and Rho signaling in cancer cell motility in 3D substrates. Oncogene 2009;28(13):1570–83.
[43] Sahai E, Marshall CJ. Differing modes of tumour cell invasion have distinct requirements for Rho/ROCK signalling and extracellular proteolysis. Nat Cell Biol 2003;5(8):711–9.
[44] Gonen-Wadmany M, Oss-Ronen L, Seliktar D. Protein–polymer conjugates for forming photopolymerizable biomimetic hydrogels for tissue engineering. Biomaterials 2007;28(26):3876–86.
[45] Almany L, Seliktar D. Biosynthetic hydrogel scaffolds made from fibrinogen and polyethylene glycol for 3D cell cultures. Biomaterials 2005;26(15):2467–77.
[46] Dikovsky D, Bianco-Peled H, Seliktar D. The effect of structural alterations of PEG-fibrinogen hydrogel scaffolds on 3-D cellular morphology and cellular migration. Biomaterials 2006;27(8):1496–506.
[47] Ghosh K, Pan Z, Guan E, Ge S, Liu Y, Nakamura T, et al. Cell adaptation to a physiologically relevant ECM mimic with different viscoelastic properties. Biomaterials 2007;28(4):671–9.
[48] Dutta RC, Dutta AK. Cell-interactive 3D-scaffold; advances and applications. Biotechnol Adv 27(4):334–339.
[49] Lutolf MP. Artificial ECM: expanding the cell biology toolbox in 3D. Integr Biol 2009;1:234–41.
[50] Harley BA, Kim HD, Zaman MH, Yannas IV, Lauffenburger DA, Gibson LJ. Microarchitecture of three-dimensional scaffolds influences cell migration behavior via junction interactions. Biophys J 2008;95(8):4013–24.
[51] Deisboeck TS, Berens ME, Kansal AR, Torquato S, Stemmer-Rachamimov AO, Chiocca EA. Pattern of self-organization in tumour systems: complex growth dynamics in a novel brain tumour spheroid model. Cell Prolif 2001;34(2):115–34.
[52] Gordon VD, Valentine MT, Gardel ML, Andor-Ardo D, Dennison S, Bogdanov AA, et al. Measuring the mechanical stress induced by an expanding multicellular tumor system: a case study. Exp Cell Res 2003;289(1):58–66.
[53] Beadle C, Assanah MC, Monzo P, Vallee R, Rosenfeld SS, Canoll P. The role of myosin II in glioma invasion of the brain. Mol Biol Cell 2008;19(8):3357–68.
[54] Lammermann T, Bader BL, Monkley SJ, Worbs T, Wedlich-Soldner R, Hirsch K, et al. Rapid leukocyte migration by integrin-independent flowing and squeezing. Nature 2008;453(7191):51–5.